

## ATTITUDE CONTROL SYSTEM OF THE EU:CROPIS MISSION

**Ansgar Heidecker**

DLR Institute of Space Systems, Bremen, Germany, ansgar.heidecker@dlr.de

**Takahiro Kato**

DLR Institute of Space Systems, Bremen, Germany, kato.takahiro@dlr.de

**Olaf Maibaum**

DLR Simulation and Software Technology, Braunschweig, Germany, olaf.maibaum@dlr.de

**Matthew Hölzel**

University of Bremen, Germany, hoelzel@uni-bremen.de

The Eu:CROPIS (Euglena Combined Regenerative Organic food Production In Space) satellite, scheduled for launch in 2017, is the next mission to be launched as part of the German Aerospace Center's (DLR) compact satellite program. The mission is currently in Phase C and is being developed jointly by several institutes within DLR. The mission's focus is to test several biological experiments at different levels of artificial gravity. The payload modules are provided by different DLR institutes, the University of Erlangen and NASA-AMES. The satellite itself has a mass of about 230 kg and includes several subsystems which directly interfere with the attitude control system (e.g. deployable solar panels, liquid pumps and venting devices). This paper provides an overview of the Eu:CROPIS Attitude and Orbit Control System (AOCS). It starts by presenting the design driving requirements and explains how the required g-levels are achieved purely by a magnetic spin stabilization concept. Following this is a presentation of the AOCS modes and a discussion of the chosen sensors and actuators. The attitude determination and attitude control algorithms are then described. Finally, an outlook is given for further development steps of the Eu:CROPIS satellite.

I. INTRODUCTION

The German Aerospace Center (Deutsches Zentrum für Luft- und Raumfahrt e.V. - DLR) is currently developing a satellite platform to carry out its own research activities within the low earth orbit environment. This satellite platform is named DLR Compact Satellite and shall serve as an object of research for satellite technologies and as a platform to support scientific payloads.

The DLR Compact Satellite program is lead by DLR's Institute of Space Systems (Bremen, Germany) and promotes the scientific excellence of DLR within a national and international framework. Therefore national and international partners with their experiments are part of the Compact Satellite. The program will lay the foundation for DLR's own technology development and establish and end-to-end system competence for scientific missions within DLR.

The term "compact satellite" refers to a satellite which dimensions are limited to an envelope of approximately one cubic meter and a maximum mass of approximately 200 kg. It should be clarified at this point that it is not planned to define any default configuration of the satellite platform itself. Instead the satellite will be developed individually according to mission specific requirements. This

is achieved by using standard components and DLR internal skills and technologies.

The objective is to implement an optimal configuration in a cost and time efficient manner. Under these guidelines, the configuration of each DLR compact satellite will be based substantially on the payload requirements and may vary extremely depending on the respective mission.

The first usage of DLR's Compact Satellite is the Eu:CROPIS mission [1], which stands for Euglena Combined Regenerative Organic food Production In Space. It is a biological payload which requires a pressurized compartment and different levels of gravity. The first part of Eu:CROPIS is a seed to seed experiment of plants under different levels of gravity. The mission goal is to provide two different levels of gravity (Moon and Mars) for six month such that the plants can go through a whole seed to seed period. During each period the plants greenhouse is connected to an algae (euglena) tank, which can neutralizing poisoning inside the greenhouse. The last element is a biological filter which can split up urine into fertiliser for the plants. The combination of these three elements, which are forming a closed loop environmental system, is the Eu:CROPIS primary payload. The euglena experiment side is provided by University of Erlangen (Erlangen, Germany) and the plant and filter side is provide by DLR Institute of Aerospace

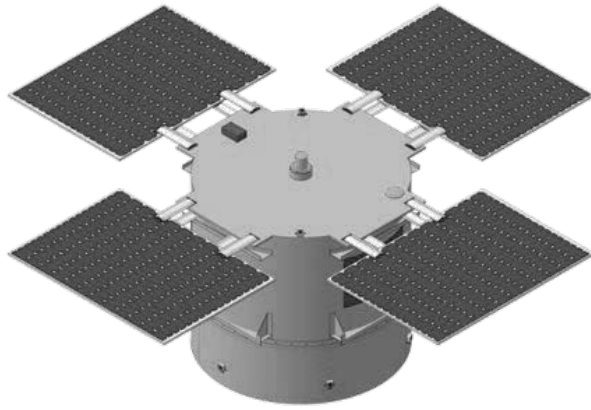


Fig. 1. Eu:CROPIS the first Compact Satellite of DLR in its deployed configuration

Medicine (Cologne, Germany).

In addition to the primary payload, which drives the mission, two secondary payloads are part of the Eu:CROPIS mission. One is provided by NASA-AMES which will carry out photosynthesis experiments and a power cell experiment. Another secondary payload consists of two radiation detectors from DLR Institute of Aerospace Medicine. One detector is inside the Eu:CROPIS payload and another one outside of the satellite exposed to the free space environment. Both detectors will give information about the radiation levels to which the payload and the satellite is exposed.

The compact satellite which was designed around these payloads can be seen in figure 1. It is a spin stabilized system with deployable solar panels. The overall dimensions are roughly 1.1 m height and 1.0 m diameter with a mass of 230 kg. It will be placed into a low earth sun synchronous orbit by a Falcon 9 rocket in 2017. The whole Eu:CROPIS mission is currently in Phase C.

## II. DESIGN DRIVING REQUIREMENTS

In general it was defined for the whole Eu:CROPIS project that only the primary payload shall drive the satellite bus design. For the AOCS this results in the major design driver to provide different levels of accelerations on a defined reference radius. This is related to the fact that the whole experiment is based on testing effects of gravity. The AOCS shall achieve acceleration levels between  $a_{min} = 0.01g$  and  $a_{max} = 0.38g$  at the primary payload reference radius of  $r = 0.35m$ . The upper limit is given by the Mars environment and the lower limit defines a minimum gravity level at which the satellite bus is considered as stabilized and the payload can start the experiments. Translated

into a rotation rate this is

$$\begin{aligned} \omega &= \sqrt{\frac{a}{r}} & (1) \\ \omega_{min} &= 5.06 \text{ rpm} \\ \omega_{max} &= 31.16 \text{ rpm} \end{aligned}$$

It should be stated clearly that the payload does not have any requirements for the orientation of the spin axis. The orientation is only driven by the power sub system. Which requires to keep the solar panel normal oriented toward the sun within a half cone of 10 degrees, during nominal mission.

In addition, the power sub system defines the maximum time of the initial detumbling and acquisition phase. This time is required to be less than four hours. Which is directly linked to the battery size.

## III. OPERATIONAL MODES

The core functions of the Eu:CROPIS AOCS are attitude and orbit determination and attitude control. To achieve the requirements the AOCS strategy is to utilize a spin stabilized concept, where the angular momentum vector is pointing to the Sun. The spin axis is the major moment of inertia axis, such that the motion itself is asymptotically stable. The angular momentum pointing can not provide long term stability due to the fact that the spin axis is not necessary parallel to the orbit normal [2]. Out of this reason the stability is achieved by a high-spin concept, where the satellite spins at several revolutions per minute (rpm). This concept fits to the acceleration requirements, due to the fact that zero gravity is not required, but it introduces a minimum level of acceleration which is necessary to achieve stability. In addition a permanent precession maneuver of roughly 1 deg/day shall be performed to keep the spin axis pointed toward the Sun.

To keep the AOCS concept as simple as possible five different control modes are defined which fully define the state of the AOCS. An overview of the modes and their interconnections can be seen in figure 2. All AOCS modes will be implemented into a well proven AOCS software framework, which was already used in former DLR projects. Each mode will utilize at least one control law which is executed at a certain frequency. The control frequency is at least ten times higher than the maximum spin frequency which is at around 0.5 Hz. To ensure a good frequency response a control frequency of 5 Hz is chosen.

### III.I. AOCS\_SFM Safe Mode

This mode captures all abnormal behavior of the AOCS. It is activated when the Failure Detection Isolation and Recovery (FDIR) system observes some error functionality. The goal of this mode is to keep the solar panels oriented

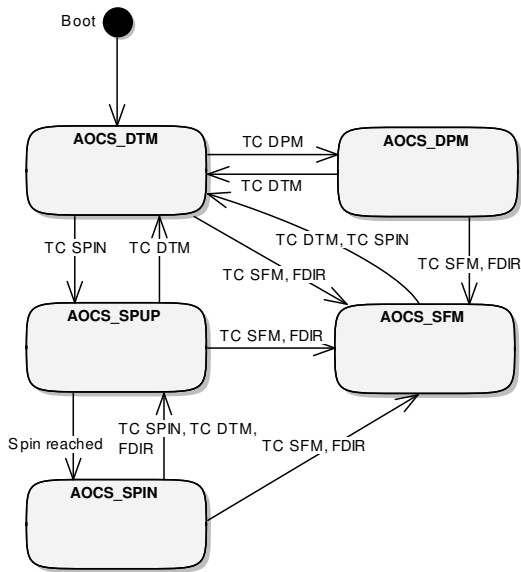


Fig. 2. Attitude Control System Modes with their possible transition

toward the sun and collect housekeeping data for further failure recovery with the ground station in the loop. In addition, the safe mode can be triggered by the satellite which sets the AOCS into a minimum power mode.

### III.II. AOCS\_DTM Detumbling Mode

This mode is activated after separation from the launcher. It is the first mode after the AOCS boots up. It reduces the remaining spin rates to a certain limit and switches into the AOCS\_SPUP when the rates are damped sufficiently.

### III.III. AOCS\_DPM Deployment Mode

This mode is used to indicate that the AOCS is ready for solar panel deployment. It can handle different moment of inertia configurations and recovers a minimum spin rate after solar panel deployment.

### III.IV. AOCS\_SPUP Spin Up/Down Mode

This mode is used to change the spin rate around the z-axis. It is used to indicate that currently an angular rate change is performed. During nominal operation it is used when a switch from one to another gravity level is performed.

### III.V. AOCS\_SPIN

This mode is used to indicate that a desired spin rate is reached and the solar panels are oriented toward the sun. Inside this mode nominal payload operation takes place. In addition a permanent precession maneuver is performed

Amount	Hardware	Key figure
3	Magnetic Torquer	30 Am <sup>2</sup>
1	Nutation Damper	liquid
2	Magnetometer	noise < 1000 nT (3 $\sigma$ )
10	Sun sensor	noise < 0.3 deg (3 $\sigma$ )
4	Angular Rate Gyroscope	RW 0.08 deg/ $\sqrt{h}$ , Bias 9 deg/h (3 $\sigma$ )
2	GPS-Receiver	DLR-Phoneix

Table 1. Attitude control system hardware devices

to keep the sun vector parallel to the spin axis over the mission time. This precession maneuver is basically a spin axis reorientation of 1 deg/day.

## IV. ACTUATORS AND SENSORS

Looking at different sensors and actuator concepts it turned out that an active magnetic attitude control scheme can fulfill the requirements. The major advantage of such a system is its simple and cost efficient design. Nevertheless it is still a challenge to design, build and operate it. Three orthogonal arranged magnetic torquers are used as actuators. They can spin up the satellite and provide sufficient torque to compensate external disturbances. The key issue during the selection of the magnetic torquers is the step response time which has to be short enough to allow the maximum rotation rate. In addition to the magnetic torquers a passive nutation damper is build into the satellite to provide a sufficient damping of unknown nutation. Two cold redundant magnetometers are used as sensors which can measure the geomagnetic field. They are based on the AMR effect which results in a much more cost effective design than a flux gate technology. Additionally several sun sensors are used which are able to provide two axis information of the Sun direction. Inertial angular rates are measured by a set of four fiber optic rate gyros which undergo a delta qualification to meet DLR internal quality assurance requirements. GPS-Receivers from DLR are used as main navigation sensor. A summary of all sensors and actuators with their key figures can be seen in table 1.

## V. ATTITUDE DETERMINATION

An Unscented Kalman Filter (UKF) approach [3], [4] is at the core of the attitude determination. The filter should be designed for a spin stabilized satellite. In [5] and [6] several Extended Kalman Filters (EKF) were developed for a spin stabilized satellite. We adopted the concept from these papers and put it into the UKF framework. The idea is to adopt the dynamic equations and the measurement models within a UKF framework to allow the filter to deal

with much longer measurement intervals than the EKF. This property is an inherent concept of the UKF which is able to capture non-linearity up to second order exactly and higher order non-linearity partly. This method emerged from the operation in eclipse. During satellite operation it will occur that the satellite is inside the eclipse and the sun sensors can not be used. If you imagine an error within the rate gyros as well the only sensor on board is a magnetometer. Therefore the UKF has to bridge gaps of roughly 20 minutes only based on magnetometer measurements.

As the system state vector we are using Markleys variables [7]

$$\mathbf{x} = [\mathbf{L}^{bf} \mathbf{L}^i \zeta]^T \quad (2)$$

which are consisting out of the angular momentum vector  $\mathbf{L}$  within the inertial and the body fixed frame respectively indicated with superscripts of  $^i$  and  $^{bf}$ . The angle  $\zeta$  describes the current rotation around the angular momentum vector. Based on this state it is possible to reconstruct a full three axis attitude information (see Appendix). For the UKF a process model

$$f(\mathbf{x}) = \dot{\mathbf{x}} \quad (3)$$

is required. These are the differential equations of the state vector which are given through [5]

$$\dot{\mathbf{L}}^{bf} = \mathbf{n}^{bf} - (\mathbf{I}^{-1} \mathbf{L}^{bf}) \times \mathbf{L}^{bf} \quad (4)$$

$$\dot{\mathbf{L}}^i = \mathbf{n}^i \quad (5)$$

$$\begin{aligned} \dot{\zeta} = & (1 + \hat{\mathbf{L}}^{bf} \cdot \hat{\mathbf{L}}^i)^{-1} [(\hat{\mathbf{L}}^{bf} + \hat{\mathbf{L}}^i) \cdot \omega_{bf,i}^{bf} \\ & + L^{-1}(\hat{\mathbf{L}}^{bf} \times \hat{\mathbf{L}}^i) \cdot (\mathbf{n}^{bf} + \mathbf{n}^i)]. \end{aligned} \quad (6)$$

In addition to the process model the measurement models are required. On board of the Eu:CROPIS satellite there are three different sensor information available angular rate  $\omega$ , geomagnetic field  $\mathbf{B}$  and sun sensor  $\mathbf{S}$  measurements. As preliminary measurement model all of these information is included into the measurement model

$$h(\mathbf{x}) = [\omega_{bf,i}^{bf} \mathbf{B}^{bf} \mathbf{S}^{bf}]^T. \quad (7)$$

At the current development stage it is assumed that the sensors are mounted in parallel to the body fixed axis and do not provide any redundant information. This is a simplification which has to be removed later but gives us the possibility to evaluate the algorithms without knowing exactly where and how the sensors are mounted inside the final satellite.

The construction of the angular rate measurements from the state vector is linked directly through the angular momentum of the satellite and the moment of inertia  $\mathbf{I}$

$$\omega_{bf,i}^{bf} = \mathbf{I}^{-1} \mathbf{L}^{bf}. \quad (8)$$

While the geomagnetic field and sun sensor measurements require a full three axis attitude information to be reconstructed

$$\mathbf{B}^{bf} = \mathbf{A}_i^{bf} \mathbf{B}^i \quad (9)$$

$$\mathbf{S}^{bf} = \mathbf{A}_i^{bf} \mathbf{S}^i \quad (10)$$

with  $\mathbf{A}_i^{bf}$  as the attitude matrix which transforms an inertial vector into a body fixed one.

All of these equations were combined with a square root UKF implementation [8] inside Matlab/Simulink for preliminary evaluation.

## V.I. UKF TUNING

In addition to the implemented process and measurement model any Kalman filter requires to define the covariances of the process  $\mathbf{Q}$  and the measurements  $\mathbf{R}$ . The covariances are linked to the squares of the standard deviation  $\sigma_x$  ( $x = \text{gyro, mag, sun}$ ). They were defined as

$$\sigma_{L^{bf}} = 2 \cdot 10^{-6} \text{ Nms}$$

$$\sigma_{L^i} = 2 \cdot 10^{-1} \text{ Nms}$$

$$\sigma_{\zeta} = 0.01 \text{ deg}$$

$$\sigma_{gyro} = 0.01 \text{ deg/s}$$

$$\sigma_{mag} = 1 \mu T$$

$$\sigma_{sun} = 0.01$$

and lead to the following covariance matrices

$$\mathbf{Q} = \text{diag}([\sigma_{L^{bf}}^2 \sigma_{L^i}^2 \sigma_{\zeta}^2]) \quad (11)$$

$$\mathbf{R} = \text{diag}([\sigma_{gyro}^2 \sigma_{mag}^2 \sigma_{sun}^2]). \quad (12)$$

which are only populated on its main diagonal.

Especially for the UKF framework three more fine tuning parameters are defined

$$\alpha = 3$$

$$\beta = 2$$

$$\kappa = 0$$

Here it is worth to note that  $\alpha$  is chosen quite high to be able to capture higher non-linearities. The alpha parameter is defining the spread of the sigma points and therefore directly effects the ability to capture non-linearities.

## V.II. SIMULATION

Based on the previous UKF definition several simulations were and are carried out. Therefore figure 3 can only give a snapshot of the current development. This figure shows the performance of the UKF at a g-level of 0.38g. The first diagram shows the error angular rate over time and the lower one the full three axis error quaternion, where the largest element is near 1 and not displayed. It can be seen that it takes some time to settle the UKF but finally reaches a sufficient accuracy.

## VI. ATTITUDE CONTROL

As baseline design the attitude control utilizes three different controllers. They face the fact that only two independent axes can be controlled at the same time. This is an inherent problem with purely magnetic attitude control and can only be addressed when the external magnetic field is changing. For Eu:CROPIS this is achieved via a near polar sun synchronous orbit. This orbit directly provides a changing external geomagnetic field which is used to achieve a control authority on all three axis over time.

To save some power and do not perform unnecessary control actuation each control torque  $\mathbf{T}_{ctrl}^{bf}$  can be transformed into a dipole moment  $\mathbf{D}^{bf}$  which does not produce any additional disturbance torques [9] via

$$\mathbf{D}^{bf} = \frac{\mathbf{B}^{bf} \times \mathbf{T}^{bf}}{|\mathbf{B}^{bf}|^2}. \quad (13)$$

The mapping is depending on the current geomagnetic field vector  $\mathbf{B}^{bf}$  and results inside a dipole which represents as good as possible the control torque. Keeping in mind this transformation the three different controllers are defined as follows.

Directly after separation from the launch vehicle a classical B-dot controller [10] is used. Its control law is defined as

$$\mathbf{D}^{bf} = -sgn(\dot{\mathbf{B}}^{bf}) \quad (14)$$

It requires only to determine the derivatives of the measured magnetic field  $\dot{\mathbf{B}}^{bf}$  which directly defines the magnetic dipole  $\mathbf{D}^{bf}$  of the magnetic torquers. This controller decreases the initial rotation rate to a minimum, such that the next controller can take over. It is still under discussion to modify this very simple and robust B-dot controller such that it e.g. damps only rotation rates around x and y axis instead of the z axis. This could help to speed up the initial sun acquisition phase.

The second controller addresses the rotation rate of the satellite. It is a simple proportional control law which directly effects the angular rate. It defines the required control torque  $\mathbf{T}_{ctrl}^{bf}$  as

$$\mathbf{T}_{ctrl}^{bf} = -K\omega_{bf,i}^{bf} \quad (15)$$

based on a strictly positive control gain  $K$  and and the angular rate  $\omega_{bf,i}^{bf}$ . To use this control law it is required to determine the three-axis angular rate and transform the control torque into a commendable magnetic dipole as describe in equation 13.

The third controller is a precession controller which takes care of the orientation of the spin axis. It is used during initial sun acquisition and to keep the solar panels oriented toward the sun during nominal operation. For defining a

precession control the satellite is treated as an already spinning system and the angular momentum vector is parallel to the major moment of inertia axis. To change the orientation of the angular momentum vector a torque has to be given which is orthogonal to the spin axis and the desired direction.

$$\mathbf{T}^{bf} = -K \frac{\mathbf{L}^{bf} \times (\mathbf{L}^{bf} \times \mathbf{S}^{bf})}{|\mathbf{L}^{bf}|^2 |\mathbf{S}^{bf}|} \quad (16)$$

This control law performs a slew maneuver, which drives the angle between the sun vector  $\mathbf{S}^{bf}$  and the angular momentum vector  $\mathbf{L}^{bf}$  to zero. In principal it mimics controllers which are typically used to reorient a spin stabilized system via thruster firing except that it is actuating permanently instead of just at discrete times. The cross products operations are used to construct a vector which lays inside the same plane as the angular momentum and the sun vector but is at the same time orthogonal to the angular momentum.

The combination of these three control laws makes it possible to achieve the desired performance. For preliminary analysis a simulation was carried out which shows the typical initial sun acquisition phase.

Figure 4 shows a result of the complete chain of the initial acquisition phase. The x-axis range is four hours which is the allowed time until the spin axis and with it the solar panels shall point toward the sun. The first diagram shows the current angular rate, the second the angle between solar panel normal and sun direction and the last diagram is the current dipole command for magnetic torque actuation. During the whole sequence the satellite is already considered as deployed. At first the B-dot controller is active which can be seen directly as the magnetic dipoles are driven to saturation. When the angular rates are damped the spin controller takes over which generates a spin around the major moment of inertia axis. After this the precession controller is switched on in parallel to the spin controller. The result is that the solar panel normal is going to align with the sun vector.

There is still a lot of space for improvements and tuning but up to now these three controllers are laying the foundation for further development. At the current development stage they have demonstrated their functionality but further they have to be tuned and tested for all different environmental conditions.

## VII. CONCLUSION AND OUTLOOK

This paper gave an overview of the current development stage of the attitude control system of the Eu:CROPIS satellite. This satellite is the first Compact Satellite of DLR. As AOCS concept a magnetic spin stabilization was choose. It is based on a typical set of actuators and sensors. As attitude determination algorithm an Unscented Kalman Filter

forms the basis. The attitude controllers are separated into three independent parts. A classical B-dot rate damping controller, a proportional spin control law and a precession controller. All AOCS functionality is implemented within a software framework that uses five different AOCS modes. Currently the whole project is inside Phase C and the AOCS development is going on. The further steps are foreseen as a twofold: the one is to improve the AOCS algorithms with the simulator and the other is the verification of the actual AOCS hardware.

## VIII. APPENDIX

### VIII.I. THREE AXIS ATTITUDE INFORMATION

To reconstruct a full three axis attitude information the following formulas were used. They are described in detailed in [5] and repeated here only for reference. The full three axis attitude matrix  $A_i^{bf}$  which transforms a vector from inertial to body fixed frame is given by

$$A_i^{bf} = R(\hat{\mathbf{L}}^{bf}, \zeta) R_i^{bf} \quad (17)$$

with

$$R_i^{bf} = (\hat{\mathbf{L}}^{bf} \cdot \hat{\mathbf{L}}^i) I_{3 \times 3} - \hat{\mathbf{L}}^i \hat{\mathbf{L}}^{bf,T} + \hat{\mathbf{L}}^{bf} \hat{\mathbf{L}}^{i,T} + \frac{(\hat{\mathbf{L}}^{bf} \times \hat{\mathbf{L}}^i)(\hat{\mathbf{L}}^{bf} \times \hat{\mathbf{L}}^i)^T}{1 + \hat{\mathbf{L}}^{bf} \cdot \hat{\mathbf{L}}^i} \quad (18)$$

$$R(\hat{\mathbf{L}}^{bf}, \zeta) = (\cos \zeta) I_{3 \times 3} + (1 - \cos \zeta) \hat{\mathbf{L}}^{bf} \hat{\mathbf{L}}^{bf,T} - \sin \zeta [\hat{\mathbf{L}}^{bf} \times] \quad (19)$$

The first transformation matrix  $R_i^{bf}$  takes the inertial angular momentum vector exactly into the body fixed angular momentum vector. The second rotation matrix  $R$  is then performing a rotation around the body fixed angular momentum vector. Therefore the attitude matrix  $A_i^{bf}$  and the first transformation matrix  $R_i^{bf}$  can transform the angular momentum vector between inertial and body fixed frame exactly, while only the full attitude matrix can transform any vector between the two coordinate systems.

## REFERENCES

- [1] DLR, German Aerospace Center (DLR), Institute of Space Systems, *Eu:CROPIS - growing tomatoes in space*, April 2014.
- [2] P. C. Hughes, *Spacecraft attitude dynamics*. J. Wiley, 1986.
- [3] S. Julier and J. Uhlmann, "Unscented filtering and nonlinear estimation," *Proceedings of the IEEE*, vol. 92, no. 3, pp. 401–422, 2004. see [11] for some corrections.

- [4] S. J. Julier, J. K. Uhlmann, and H. F. Durrant-Whyte, "A New Approach for Filtering Nonlinear Systems," in *Proceedings of the American Control Conference*, (Seattle WA, USA), p. 1628–1632, 1995.
- [5] F. L. Markley and J. E. Sedlak, "Kalman Filter for Spinning Spacecraft Attitude Estimation," *Journal of Guidance, Control and Dynamics*, vol. 31, no. 6, pp. 1750–1760, 2008.
- [6] J. E. Sedlak, "Kalman Filter Estimation of Spinning Spacecraft Attitude Using Markley Variables," in *18th International Symposium on Space Flight Dynamics*, (Munich, Germany), October 2004.
- [7] F. L. Markley, "New dynamic variables for rotating spacecraft," in *International Symposium on Space Flight Dynamics*, vol. 84 of *Advances in the Astronautical Sciences*, (Greenbelt, MD), NASA/GSFC, Univelt, Inc., April 1993.
- [8] R. van der Merwe, *Sigma-Point Kalman Filters for Probabilistic Inference in Dynamic State-Space Models*. PhD thesis, Oregon Health & Science University, 2004.
- [9] M. J. Sidi, *Spacecraft Dynamics and Control*. Cambridge Aerospace Series, Cambridge University Press, 1997.
- [10] A. C. Strickler and K. T. Alfriend, "Elementary Magnetic Attitude Control System," *Journal of Spacecrafts and Rockets*, vol. 13, pp. 282–287, May 1974.
- [11] S. Julier and J. Uhlmann, "Corrections to [3]," *Proceedings of the IEEE*, vol. 92, no. 12, pp. 1958–1958, 2004.

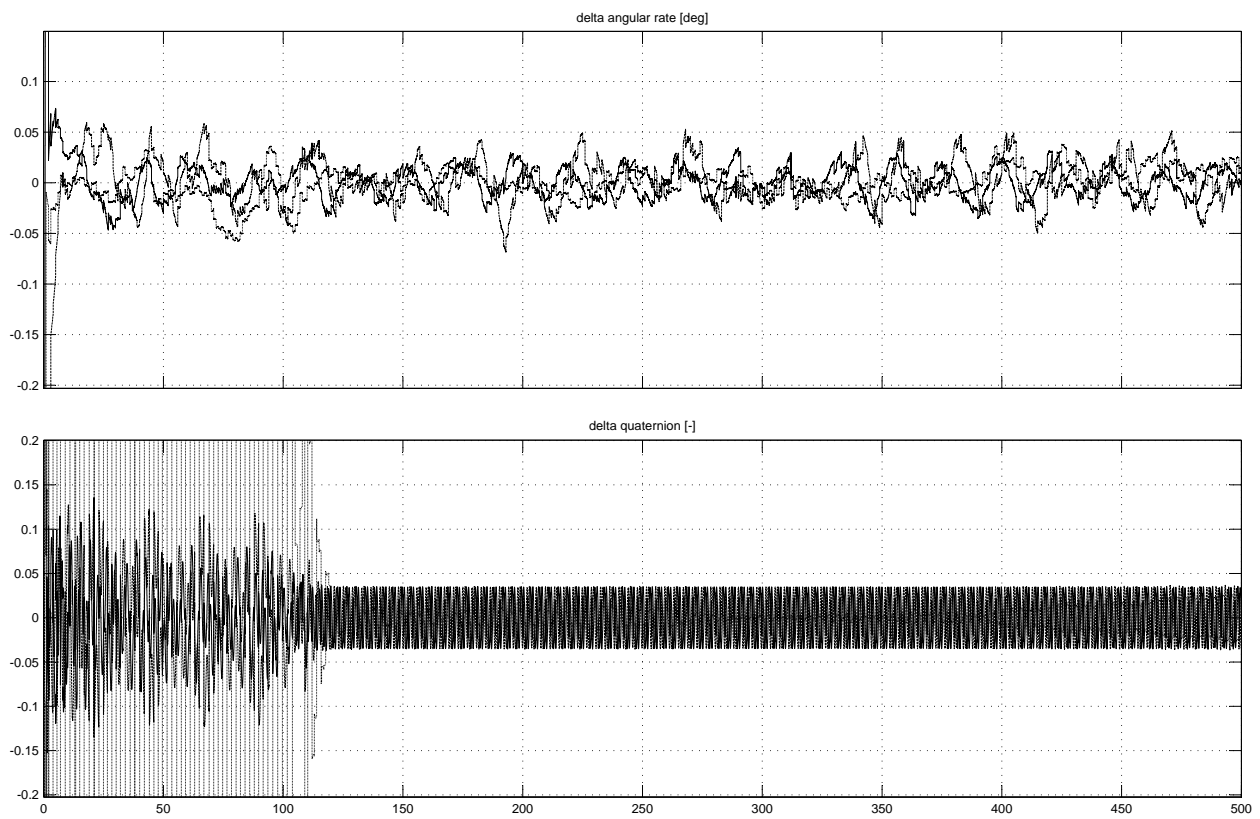


Fig. 3. Typical attitude determination error based on an unscented kalman filter.

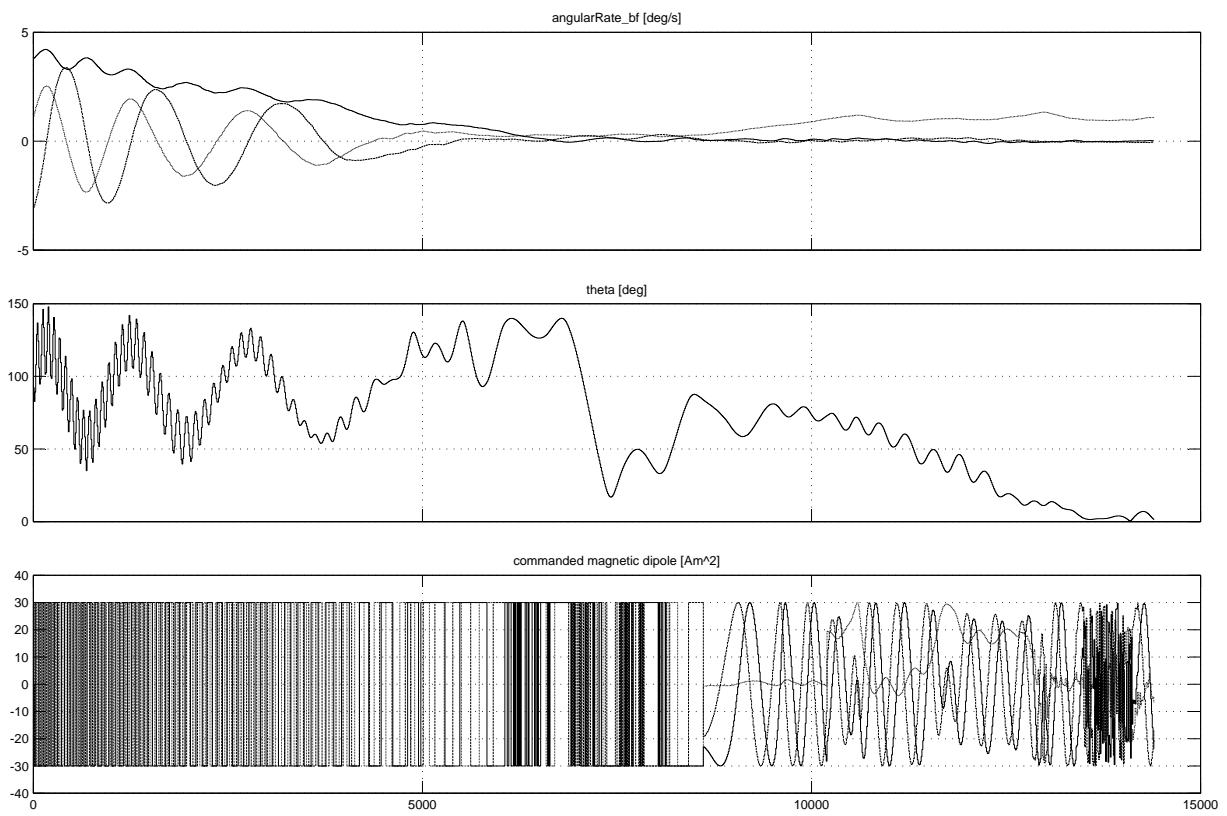


Fig. 4. Simulated initial detumbling and sun acquisition of the Eu:CROPIS satellite.